

## Fatigue Life of the Repair TIG Welded Hastelloy X Superalloy

Restu SIHOTANG\*, Sang-Kyu CHOI\*\*, Sung-Sang PARK\*\*\* and Eung-Ryul BAEK\*\*\*,†

\*Research and Development Center, KOS Limited, Yangsan 626-230, Korea

\*\*HYUNDAI BNG STEEL, Changwon 642-370, Korea

\*\*\*School of Materials Science and Engineering, Yeungnam Univ, Gyeongbuk 712-749, Korea

†Corresponding author : erbaek@yu.ac.kr

(Received July 21, 2015 ; Revised August 17, 2015 ; Accepted August 26, 2015)

### Abstract

Hastelloy X in this study was applied in jet engine F-15 air fighter as shroud to isolate the engine from outer skin. After 15 years operation at elevated temperature the mechanical properties decreased gradually due to the precipitation of continuous second phases in the grain boundaries and precipitated inside the grain. The crack happened at the edge of the shroud due to the thermal and mechanical stress from jet engine. Selective TEM analysis found that the grain boundaries consist of  $M_{23}C_6$  carbide,  $M_6$  Ccarbide and small percentage of sigma( $\sigma$ ) phase. Furthermore, it was confirmed the nano size of  $\sigma$  and  $\mu$  phase inside the grain.

In this study, it was investigated the microstructure of the degraded shroud component and HAZ of repair welded shroud. In the HAZ, it was observed the dissolution of the  $M_{23}C_6$  carbides and smaller precipitates, the migration of the undissolved larger  $M_{23}C_6$  carbide and  $M_6$  Ccarbide. It is also observed the liquation due to the simply melt of the segregated precipitates in the grain boundaries. Interestingly, the segregated second phases which simply melt in the grain boundaries more easily happened at higher heat input welding condition. High temperature tensile test was done at 300°C, 700°C and 900°C. It was obtained that the toughness of welded sample is lower compare to the non-welded sample.

The solution heat treatment at 1170°C for 5 minutes was suggested to obtain a better mechanical properties of the shroud. The high cycle fatigue number of the repair welded shroud shows a much lower compare to the shroud. In addition, the high cycle fatigue number at room temperature after solution heat treatment was almost double compare to the before solution heat treatment under 420-500MPa stress amplitude. However, the high cycle fatigue number of repaired welded sample was shown a much lower compare to the non-welded shroud and solution treated shroud. One of the main reasons to decrease the tensile strength and the high cycle fatigue properties of the repair welded shroud is the formation of the liquid phase in HAZ.

Key Words : Superalloy, Hastelloy X, Grain boundary liquation, High cycle fatigue test.

### 1. Introduction

Hastelloy-X is a Ni-base superalloy and widely used in aerospace and nuclear industries due to its high corrosion resistance and good strength in elevated temperature. Commercial Hastelloy X consists of coarse  $\gamma$  grain and Molybdenum rich carbide ( $M_6C$ ). The carbide volume fraction is less than 1 % as reported by Baek E et al.<sup>1)</sup> Shroud is a thermal barrier in jet engine F-15 air fighter

and usually exposed to a high temperature for about 15 years operation. This material is made of Hastelloy X superalloy based on the composition and the mechanical properties are extremely degraded after suffering in high temperature for a long time. The thermomechanical degradation of the shroud was intensively investigated by Baek E. et al.<sup>1)</sup> and it was found that the precipitated carbides acted as the origin of the crack initiation site. In a separated work, which has been reported elsewhere,<sup>2-6)</sup> precipitation of intermetallic compounds  $\rho$ ,  $\mu$  and carbides have

been observed in commercial grade of superalloy at a different aging condition.

<sup>a</sup> Aging is a very important process which is used for the manufacturing of and repaired crack of shroud. The crack generally happened at the edge of shroud due to the thermal and mechanical stress from jet engine operation to degrade shroud component. <sup>c</sup> Furthermore, owing to the high cost of the shroud, it is economically more viable to repair the degraded component than to replace <sup>b</sup> m with a new part. Welding is required to repair the crack in the degraded component, but it is known that the properties of weld zone (WZ) and heat affected zone (HAZ) are inferior to the wrought shroud properties. The inferiority of WZ of some superalloy materials are originated from brittle close-packed (TCP) phases as investigated by some researchers.<sup>2,3,7-10)</sup>

Fabrication and repair of shroud are performed using conventional Tungsten inert gas (TIG) welding. Nevertheless, the high heat input generates a huge effect on the HAZ resulting in the grain growth and melting of eutectic constituents.<sup>11,12)</sup>

This study focuses on the investigation of fatigue and high temperature tensile properties of repaired crack shroud by TIG welding.

## 2. Experiment

The shroud was provided by the Institute of Aviation Technology, South Korea. It is 0.7 mm thick and chemical composition is given in table. 1. This material has been used for almost 15 years as a thermal barrier in jet engine F-15 fighter. Solution treatment of shroud was done at 1175°C for 5 min in argon environment (henceforth referred to as ST shroud).

The repair welding (henceforth referred to as welded shroud) was made by TIG (with filler) and the procedure was prepared in table 2. The type of filler metal as AMS 5798 standard, 3/16 wire filler diameter. Specifically, the joint was made by butt joint.

The high temperature tensile specimen was prepared according to the ASTM E8 and was done by Zwick 10 ton class Z100 tensile tester. High cycle fatigue test at room temperature was done for shroud, welded shroud and ST shroud. High cycle fatigue test was done at frequency 50 kHz with load ratio ( $\sigma_{min}/\sigma_{max}$ ) = 0.1 and samples were prepared according to the ASTM E466. The maximum stress applied during testing was varied from 400 MPa to 520 MPa.

The basic research data were obtained by scanning electron microscope (SEM), and transmission electron microscope (TEM). A SEM Hitachi FE-SEM 4800 with 15 kV along with energy dispersive spectroscopy (EDS) analysis was utilized to examine the change of microstructure in the

**Table 1** Chemical composition (wt%) of Hastelloy X and wire filler

Element	Ni	Cr	Fe	Mo	Co	W	C	Mn	Si	B
Hastelloy X	Bal	22	18	9	1.5	0.6	0.1	1	1	0.008
Wire filler	Bal	22	19	9	1.5	0.6	0.1	1	1	0.01

**Table 2** TIG welding parameters

	I (A)	v(cm/min)	HI (kJ/cm)
LHI	15	20	7.5
HHI	20	12	16.67

\* LHI = low heat input \*HHI = High heat input

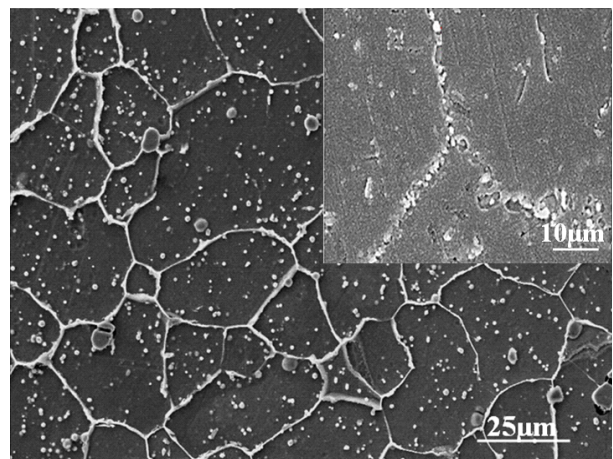
HAZ. TEM JEM-2100F HR by JEOL was introduced to examine the phases. A solution of 98 mL distilled water and 2 g perchloric acid was for electro etching. Electro etching was done by Buehler Electromet-III was operated at 3 V for 20-30 s with stainless probe as anode and graphite as cathode.

## 3. Results and Discussion

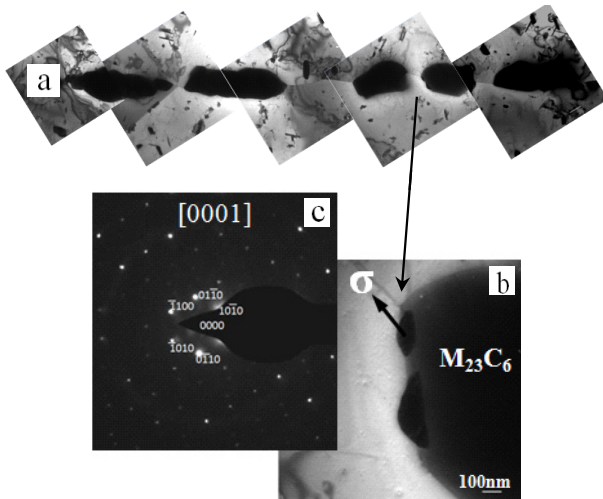
### 3.1 Microstructure of Shroud

Fig. 1 shows the SEM micrograph of shroud. The microstructure consist of equiaxed austenite grain, coarse  $M_6C$  carbides, continuous film of grain boundary carbides and TCP phases. Total volume fraction of precipitate reaches 15%. Liu et al.<sup>11)</sup> has proposed the precipitation of  $M_{23}C_6$  carbide at grain boundaries during heat treatment. Furthermore, it is well published that  $M_6C$  carbides is an unstable carbide as it can decompose to the new precipitate during aging.<sup>12,13)</sup> Bai et al.<sup>14)</sup> published that  $M_6C$  carbide can decomposed into  $M_{32}C_6$  carbide with a prolonged exposure.

After exposure in elevated temperature for a long time, the TCP phases were precipitated in the region near the



**Fig. 1** SEM micrograph of Shroud



**Fig. 2** TEM micrograph showing precipitated carbide along the grain boundary (a) ( $M_{23}C_6$ ) carbide (b)  $\sigma$  phase precipitated from  $M_{23}C_6$  carbide (c) corresponding diffraction pattern [0001]

prior carbides. Fig. 2 shows TEM observation of grain boundary precipitate consist of  $M_{23}C_6$  carbide,  $M_6C$  carbide and new  $\sigma$  phase. It can be seen that  $\sigma$  was precipitated from  $M_{23}C_6$  carbide as identified by selected area diffraction analysis in Fig. 2. EDS analysis for  $\sigma$  phase indicates that the precipitate is rich of Cr elements, and has the composition (wt%) of: Cr36.7, Mo28.5, Fe13.3, C0.46, Ni20.8.

Besides, ovate  $\mu$  phases were observed around  $M_6C$  carbide in the grain interior as shown in Fig. 3. The corresponding pattern confirms the  $\mu$  phase which has a rhombohedral crystal structure with a lattice constant  $a_{\mu} = 8.9 \text{ \AA}$ .

After solution treatment most of the precipitate was dissolved back into matrix. It was found the decreasing of precipitate by 10% after solution treatment at  $1175 \text{ }^{\circ}\text{C}$  for 5 minutes. Most of the fine  $M_{23}C_6$  carbide was dissolved into the matrix and only remain the very coarse  $M_{23}C_6$  and  $M_6C$  carbide. It was expected that the dissolution treatment of precipitate into the matrix during solution treatment promoted profuse secondary hardening.

### 3.2 Microstructure of Welded Shroud

In the previous publication<sup>8)</sup>, it was investigated the formation of intermetallic TCP phase in the WZ due to the elements segregation during solidification in subgrain level. The intermetallic was found inside the interdendritic region. A similar observation was well published by many authors.<sup>2-5,15)</sup> Perricone and DuPont<sup>7)</sup> proposed the formation of  $\sigma$  and P phase in the WZ of alloy C-22 (22%Cr, 13%Mo) by calculated multi component liquids projections and solidification modeling. It was also confirmed in the previous study<sup>8)</sup> that the formation of TCP phase in the WZ do not cause any solidification cracking inside the WZ due to the usage of proper filler metal.

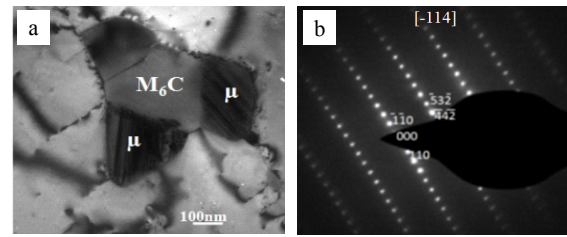


**Fig. 3** (a) TEM image of  $\mu$  phase precipitated from  $M_6C$  carbide (b) corresponding diffraction pattern [-114] axis zone.

More interestingly observation was found in HAZ. In general, the grain growth was occurring. Low heat input ( $7.5 \text{ kJ/cm}$ ) promotes the dissolution of grain boundary precipitate into the matrix. The dissolution can potentially compromise the strength of the HAZ since the temperature act as solution treatment to dissolve the precipitate into the matrix. In addition, the liquation still happened though in a very small area. The liquation happened due to the simple melt of segregated precipitate in the grain boundary. For high heat input condition ( $16.67 \text{ kJ/cm}$ ), the intergranular HAZ cracking was clearly observed. The rapid heating during welding in respect of the thermal cycle does not permit sufficient time to dissolve second phases in the grain boundaries and within the grain. Those second phases melt and form liquated products with a very low bonding strength with austenitic matrix. In the previous study, room tensile test was done and shows that low heat input sample is superior to that of high heat input samples associated with the formation of grain boundary liquid film.<sup>8)</sup> Furthermore, geometry is also one of the considerable aspects. Geometry factor is considered since the weld bead of high heat input sample is much bigger than low heat input samples.

### 3.3 High temperature tensile test and High cycle fatigue test

In this study, the high temperature tensile test was done

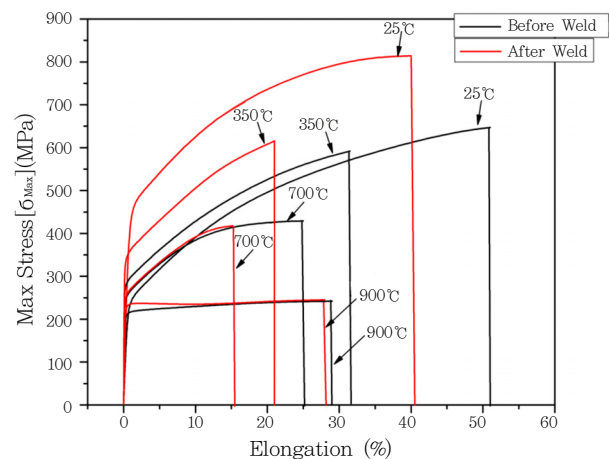


**Fig. 4** High temperature tensile test of low heat input sample

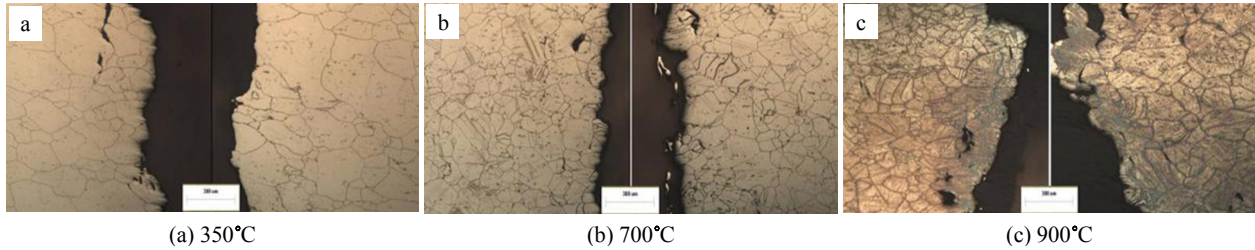


**Fig. 5** Fractographs of high temperature tensile specimens which was welded with low heat input condition failed at BM

for low heat input welded shroud and shroud. The result is shown in Fig. 4. The elongation of post-welding shroud drops significantly as the testing temperature increase. Fig. 5 shows that all samples fail in the base metal (BM). It can be deduced that WZ and HAZ of low heat input is strong enough to prevent the tensile failure in room and high temperature.

High cycle fatigue test was done to shroud, ST shroud and low heat input welded shroud. Fig. 6 shows the results of stress applied versus fatigue cycle number (S-N curve). The S-N curve shows a general trend that the fatigue life increases with decreasing cyclic stress amplitude. Note that arrow indicate that the failure of specimen did not occur during test. ST shroud shows a significant improvement in the fatigue number in comparison with the shroud. The significant effect of solution treatment can be pointed out by the dissolution of brittle precipitate during solution treatment and increase the strengthening element in the matrix. The cycle fatigue number for welded sample shows inferior though the test was done in a lower stress amplitude. Furthermore, it is suggested to apply solution treatment for used shroud before conducting a repair welding.

Fig. 7 shows the fatigue failure for  $\sigma_{max} = 240$  MPa,  $\sigma_{max} = 320$  MPa,  $\sigma_{max} = 380$  MPa and  $\sigma_{max} = 400$  MPa. All the failure was happening in the HAZ, starting from the edge of bead. The stress concentration and liquated

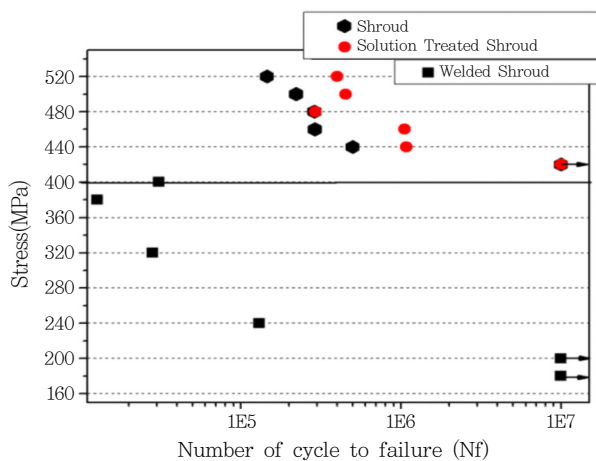


**Fig. 6** S-N curve from fatigue test of low heat input welded shroud, shroud and ST shroud.

product simultaneously cause the failed position in the HAZ. In the previous study, it was found that room temperature tensile test fractured in the base metal for low heat input sample, and in HAZ for the high heat input sample. It was proposed that the main reasons were liquation and geometrical factor. High heat input sample shows a bigger of front bead and back bead size compare to the low heat input samples and generate a higher stress concentration at the edge of bead. For high cycle fatigue test, the stress concentration at the edge of the bead should be more sensitive and cause an earlier fracture compare to the nonwelded samples. Thus, it can be pointed out that the geometrical and small liquation part is the main reason for earlier fatigue fracture on welded sample.

#### 4. Conclusions

1.  $\sigma$ -phase is precipitated from  $M_{23}C_6$  carbide in the grain boundary while  $\mu$  phase is precipitated from  $M_6C$  carbide.
2. HAZ of low heat input welded sample is strong

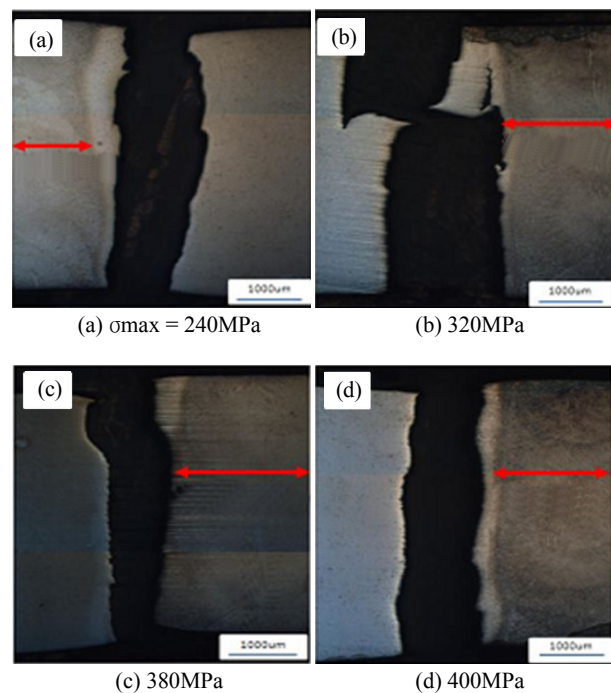


**Fig. 7** Fatigue fracture area in HAZ



enough to prevent the tensile failure at high temperature.

3. Liquation and geometry factor simultaneously cause an earlier fatigue fracture in HAZ of welded sample.

4. It is suggested to apply solution treatment before conduction a repair welding of used shroud.

### References

1. E. R. Baek, S. S. Park, R. S. Sihotang and S. K. Choi, Heat treatment of the degraded hastelloy-X for high cycle fatigue properties, *Proc. 9th Int. Conf. on Fracture and strength of solid*, 91 (2013)
2. M. J. Cieslak, T. J. Headley and A. D. Romig, Jr, The welding metallurgy of Hastelloy Alloy C-4, C-22 and C-276, *Metall. Trans. A*, 17A, 1986, 2035-2047
3. M. J. Perricone and J. N. DuPont, Effect of composition on the solidification behavior of several Ni-Cr-Mo and Fe-Ni-Cr-Mo alloys, *Metall. Mater. Trans. A*, 37A (2006), 1267-1280
4. R. B. Leonard, Thermal stability of hastelloy alloy C-276, *Corrosion*, 25 (1969), 222-228.
5. C.R. Lee, S.H.Um, S.W. Kim, and C.H.Lee: A study on hot ductility behavior of Ni-based superalloys, *Journal of KWJS*, 22-2 (2004), 157-166 (in Korean)
6. Y.S.Kim, Y.G.Choi, C.H.Lim, and J.D.Kim, A study on the abrasive wear properties of the PTA overlay layers using the super alloy powder, *Journal of KWJS*, 27-3 (2009), 80-84 (in Korean)
7. M. J. Perricone, J. N. Dupont and M. J. Cieslak, Solidification of hastelloy alloys : an alternative interpretation, *Metall. Mater. Trans. A*, 34A (2003), 1127-1132.
8. R. Sihotang, P. Sung-Sang and B.Eung-Ryul, Effect of heat input on microstructure of tungsten inert gas welding used hastelloy-X, *Material Research Innovatios.* 18 (2014), 1074-1080
9. O. A. Ojo and M. C. Chaturvedi, Liquation microfissuring in the weld heat-affected zone of an overaged precipitation-hardened nickelbase superalloy, *Metall. Mater. Trans. A*, 38A (2007), 356-369.
10. L. O. Osoba, R. K. Sidhu and O. A. Ojo, On preventing HAZ cracking in laser welded DS Rene 80 superalloy, *Mater. Sci. Technol.*, 27 (2011), 897-902.
11. Z. Tang, J. Li, R. Hu, Y. Liu, and G. Bai, Effect of solution heat treatment on carbide of Ni-Cr-W superalloy, *Rare Met. Mater. Eng.*, 39 (7) (2010), 1157-1161
12. Z. Yanping, K. Lizhong and X. Xishan, Influence of thermal exposure on the precipitates and mechanical properties of a newly developed Ni- 21Cr-17Mo alloy, *Mater. Sci. Eng. A*, 560 (2013), 611-617
13. X.Z. Qin, J.T. Guo, C. Yuan, J.S. Hou, L.Z. Zhou and H.Q. Ye, Long-term thermal exposure response of the microstructure and properties of a cast Ni-base superalloy, *Mater. Sci. Eng. A*, 543 (2012), 121-128
14. B. Guanghai, L. Jinshan, H. Rui, Z. Tiebang, K. Hongchao and F. Hengzhi, Effect of thermal exposure on the stability of carbides in Ni-Cr-W base superalloy, *Mater. Sci. Eng. A*, 528 (2011), 2339-2344
15. N. L. Richards, R. Nakkalil and M. C. Chaturvedi, The influence of electron-beam welding parameters on heat-affected-zone microfissuring in Incoloy 903, *Metall. Mater. Trans. A*, 25A (1994), 1733-1745.